Analysis X-ray absorption fine structure using absolute X-ray mass attenuation coefficients: Application to molybdenum

ARTICLE *in* RADIATION PHYSICS AND CHEMISTRY · NOVEMBER 2006

Impact Factor: 1.38 · DOI: 10.1016/j.radphyschem.2005.07.016

5 AUTHORS, INCLUDING:

L.F. Smale
University of Melbourne
15 PUBLICATIONS **82** CITATIONS
SEE PROFILE

Christopher Thomas Chantler
University of Melbourne
165 PUBLICATIONS **1,999** CITATIONS
SEE PROFILE

Martin D de Jonge
Australian Synchrotron
131 PUBLICATIONS **2,163** CITATIONS
SEE PROFILE

Zwi Barnea
University of Melbourne
98 PUBLICATIONS **1,613** CITATIONS
SEE PROFILE

Available online at www.sciencedirect.com
ScienceDirect
Radiation Physics and Chemistry 75 (2006) 1559–1563
Radiation Physics and Chemistry
www.elsevier.com/locate/radphyschem

Analysis of X-ray absorption fine structure using absolute X-ray mass attenuation coefficients: Application to molybdenum

L.F. Smale, C.T. Chantler*, M.D. de Jonge, Z. Barnea, C.Q. Tran

School of Physics, University of Melbourne, Victoria 3010, Australia

Accepted 9 July 2005

Abstract

XAFS structures are solved routinely and hundreds of publications appear per annum. Limitations in theoretical predictions and XAFS analytical frameworks lead to significant uncertainty in results. This impairs structural predictions and prevents ab initio determination. The highest accuracy experimental data have been obtained using the XERT and the most popular technique to analyse the structure. We apply an accurate χ^2 fitting procedure to the molybdenum attenuation data including error propagation and improve the XAFS determinations by between 5% and 70%.

PACS: 78.70.Dm; 61.10.Ht; 32.80.Fb

Keywords: X-ray absorption; XAFS; XANES; Molybdenum

1. Metallic molybdenum: an ideal test case for the XAFS technique

The mass attenuation coefficient data for metallic molybdenum have recently been determined to unprecedented accuracy within the range from 13.5 to 41.5 keV. Accuracy is within 0.02–0.4% and 0.1% over most of the energy range. This range includes the K edge for molybdenum (de Jonge et al., 2005). The data (Fig. 1) are on absolute scales for both the mass attenuation and X-ray energy axes. The accuracy of the energy determinations of each datum is typically 1–3 eV. This accuracy was obtained using the X-ray extended-range technique (XERT) (Chantler et al., 2001; Tran et al., 2003). The XERT tests for many potential experimental systematic errors over a large energy range, and hence offers an unprecedented opportunity to critically examine and improve the standard XAFS analysis technique and theory. These measurements obtained from molybdenum yield the most accurately determined form factor in the literature for any element or substance.

2. Issues in current XAFS analysis

The mass attenuation coefficient $[\mu/\rho]$ for a material is a function of X-ray energy given by the Beer–Lambert formula

$$I = I_0 e^{-[\mu/\rho]\rho t}. \quad (1)$$

*Corresponding author.
E-mail address: chantler@physics.unimelb.edu.au (C.T. Chantler).

0969-806X/$ - see front matter © 2006 Elsevier Ltd. All rights reserved.
doi:10.1016/j.radphyschem.2005.07.016

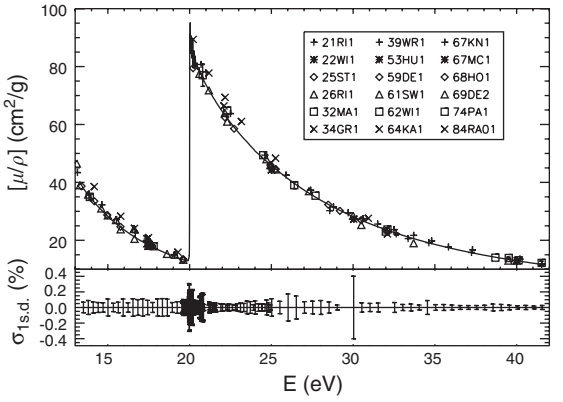

Fig. 1. $[\mu/\rho](E)$ versus E for molybdenum, compared with previous measurements sourced from the compilation of Hubbell (1994) (legends as given therein). The error bars for previous measurements are between 2% and 4%. The solid line is the recent data. The bottom section shows σ_{1sd} in the new data as a percentage of the data ranging from 0.02% to 0.4%, and generally 0.1%. This quality of data is uniquely suited to test XAFS theory.

The normalised offset XAFS spectrum, fitted by standard techniques, called $\chi(k)$, is the oscillatory part of the mass attenuation above an absorption edge as a function of the photo-electron wave number k. $\chi(k)$ is related to $[\mu/\rho](E)$ by

$$\chi(k) = \frac{[\mu/\rho](E) - [\mu_0/\rho](E)}{[\mu_0/\rho](E)}, \tag{2}$$

$$E = \frac{h^2}{8m_e\pi^2}k^2 + E_0, \tag{3}$$

where μ_0 is a smooth atom-like background and E_0 is the energy of the edge. There is currently no rigorous determination of the atom-like smooth baseline μ_0 or of the effective energy E_0 for general edges. More standard approaches simply draw a smooth line or curve through the oscillatory amplitude and normalise empirically to this. Two of the most useful atomic baselines for XAFS are Chantler (1995, 2000) and Mihelic et al. (2004). Recently, limitations of both contemporary theoretical approaches have been shown to obscure the direct interpretation of XAFS.

The XAFS equation describes this $\chi(k)$ as a sum over multiple scattering paths:

$$\chi_{\rm th}(k) = \sum_j N_j S_0^2 F_j(k) \frac{\sin[2kr_j + \phi_j(k)]}{kr_j^2} \times e^{-2\sigma_j^2 k^2} e^{-2r_j/\lambda(k)}, \tag{4}$$

where subscript j indexes the jth path, N_j is the degeneracy, S_0^2 is the many-body reduction factor, $F_j(k)$ is the backscattering amplitude function, $r_j = (1+\alpha)r_{0,j}$ is half the path length, $r_{0,j}$ is the same quantity at a reference temperature, $\phi_j(k)$ is a total phase shift function, σ_j is a Debye-Waller factor and $\lambda(k)$ is the photo-electron mean free path function.

XAFS analysis techniques use Eq. (4) as a model for XAFS. One of the best current analysis packages is IFEFFIT, an interactive shell for the FEFF code (Newville, 2001). Given an input local structure (a crystal structure at some temperature), FEFF will output N_j, $r_{0,j}$, $F_j(k)$, $\phi_j(k)$ and $\lambda(k)$ for the most dominant photoelectron scattering paths. That leaves S_0^2, σ_j and α_j undetermined for each scattering path.

This leaves freedom to model these path parameters. To good accuracy all α_j's are equal to a single parameter α. The σ_j's are modelled by the correlated Debye model with the Debye temperature $\theta_{\rm D}$ as a free parameter:

$$\sigma_j^2 = \frac{1}{4}\sum_{ij}\langle(\mathbf{u}_i - \mathbf{u}_{i+1})\cdot\hat{\mathbf{R}}_{i,i+1}(\mathbf{u}_j - \mathbf{u}_{j+1})\cdot\hat{\mathbf{R}}_{j,j+1}\rangle, \tag{5}$$

where $\mathbf{u}_i$ is the fluctuation in position of the ith atom in the path and $\mathbf{R}_{i,j}$ is the displacement from the ith atom to the jth atom in the path. This can be cast in terms of the correlation between the kth component of the $\mathbf{u}_i$ vector and the lth component of $\mathbf{u}_j$:

$$\langle u_{i,k}u_{i,l}\rangle = \frac{\hbar^2}{k_{\rm B}\theta_{\rm D}\sqrt{M_iM_j}}\int_0^1 {\rm d}w \frac{\sin(wR_{ij}k_{\rm D})}{R_{ij}k_{\rm D}}\coth\left(\frac{w\theta_{\rm D}}{2T}\right), \tag{6}$$

where $k_{\rm B}$ is Boltzmann's constant, $k_{\rm D} = (6\pi^2N/V)^{1/3}$, N/V is the number density of the crystal, T is the absolute temperature of the crystal and M_i is the mass of the ith atom in the path (Zabinski et al., 1995).

For each path $N_jS_0^2$ is a constant, so the roles of N_j and S_0^2 are not separable. A separate parameter $S_{0,j}^2$ for each path models the variation of the product. The analysis of this work focuses on propagating accurate experimental errors through a direct windowed k space fitting as this gives the most direct and transparent test of the procedure.

The accurate χ^2 (chi-squared) for χ (chi) data is

$$\chi^2 = \sum_{i=1}^{N_{\rm pts}}\left(\frac{\chi_{\rm data}(k_i) - \chi_{\rm th}(k_i)}{\sigma(k_i)}\right)^2, \tag{7}$$

where $(k_i, \chi_{\rm data}(k_i))$ is the ith data point and $\sigma(k_i)$ is the measurement uncertainty of the $\chi_{\rm data}(k_i)$. The reduced χ^2 is

$$\chi_{\rm r}^2 = \frac{\chi^2}{N_{\rm pts} - N_{\rm var}}. \tag{8}$$

We can evaluate fits generated by the standard procedure with $\chi_{\rm r}^2$ to determine the accurate goodness of fit. $\chi_{\rm r}^2$ was implemented in the core of the computation code so we fit with respect to χ^2 and evaluate the standard fits with $\chi_{\rm r}^2$.

3. Investigations and results

We report here variation of two parameters of the standard procedure: the windowing region and the parametrisation of the paths $S^2_{0,j}$ for the molybdenum model. We examined fits with the following window regions: $3.7-13.0\,\text{Å}^{-1}$ (7 peak window), $2.0-13.0\,\text{Å}^{-1}$ (8 peak window) and a range covering all the data (unwindowed). The model for molybdenum includes 16 scattering paths, the theory converging after the inclusion of these 16 paths. All 16 of the $S^2_{0,j}$'s were set equal to the one model parameter S^2_0. The figure shows that the windowed fits are of very high quality and in good qualitative agreement with the peaks and troughs of the data. No k-weighting was employed. This is a confirmation of the modified technique and of the experimental data.

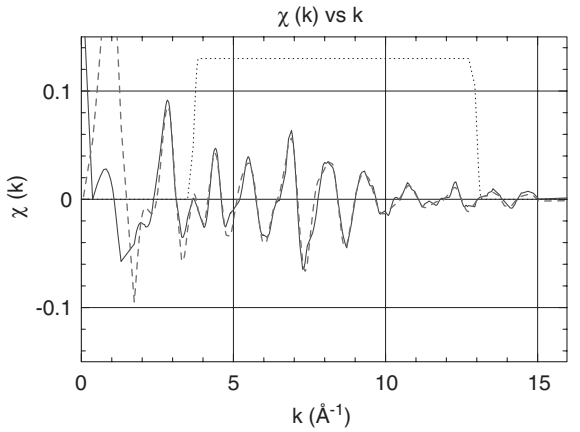

Fig. 2. The $\chi(k)$ data (solid line) and the windowed χ^2 fit using the reduced set of parameters (dashed line). The k space window function (dotted line) represents the 7 peak window. $\chi^2_r = 96$. The fit is qualitatively consistent with the data in the windowed region, matching peak locations and heights. However, the χ^2_r indicates a significant disagreement between theory and the high-accuracy experimental data. Further theoretical work is needed.

The model curves for the 7 and 8 peak windowed fits followed the experimental data with peak locations and heights being roughly consistent. However, the χ^2_r was consistently between 63 and 180 for all fits, indicating a model failure revealed by the high accuracy of the data (Fig. 2, Table 1).

The unwindowed fits had χ^2_r exceeding 2500, an order of magnitude greater than the windowed fits. All parameter values for the unwindowed fits were unphysical. Hence the model is unable to fit the XANES region. This is the traditional justification within the XAFS community of windowing: peaks in the XANES region may not be well represented by an XAFS analysis. The upper limit of the window prevents the noise level far from the edge from being too significant, especially if traditional k^3 scaling is used.

Parameter values for the 8 peak window fits were either unphysical or poorly determined. Generally the values for the Debye temperature were too low, and the values for the path amplitudes were too high. This is correlated with a higher χ^2_r, although the 8 peak window fits are obviously poor in a range where the model assumptions are not adequate. Perhaps surprisingly, we have already removed the first 4 peaks by windowing, so naively one might expect the model to work well (and it does in a qualitative sense).

Windowed fits allowing all 16 $S^2_{0,j}$'s to vary independently yielded high correlations. Although the extra

Table 1
The parameters and uncertainties from a 7 peak window fit (windowed from 3.7 to $13.0\,\text{Å}^{-1}$)

	Improved fit (7 peaks)			Standard fit (8 peaks)	Literature value
	Value	σ	$\sigma\sqrt{\chi^2_r}$		
χ^2	24 000			38 000	
χ^2_r	96			130	
E_0(eV)	19996.88	0.03	0.33	19996.21	
α	0.00183	9×10^{-5}	0.00086	−0.0003(5)	$0\pm6\times10^{-5}$
θ_D (K)	360	2	16	344(9)	385(7)
S^2_0	1.153	0.006	0.055	1.11(3)	0.9

Two estimates, σ and $\sigma\sqrt{\chi^2_r}$, give lower and upper bounds for one standard deviation uncertainty. The fit is consistent with established values to within 2–3 standard deviations. The model gives meaningful parameters with a particularly restricted window. The unit cell length is between 3.1470 and 3.1474 Å (Edwards et al., 1951; Wyckoff, 1963; Taylor et al., 1961), based on X-ray crystallography carried out between 18 and 25 °C. With the model parameter 3.1474 Å., an expected expansion coefficient of $(1+\alpha)$, $\alpha = 0.00000(6)$ follows. The Debye temperature for molybdenum is 385(7) K from powder neutron diffraction (Bashir et al., 1992).

parameters always gave an expected reduction in χ^2_r, the corresponding path amplitudes were often unphysical, implying that the amplitudes were not determined, even for such an ideal model system as pure molybdenum.

In all fits, the development of the accurate χ^2 fitting procedure including error propagation showed improvement of the XAFS determinations by between 5% and 70%. The 7 peak windowed fit yields parameter values corresponding to physical quantities. Other results, while still useful for some applications, were likely to lead to significant uncertainty in determined parameters.

Standard procedures for fitting the FEFF model to an experimental XAFS spectrum are based on a least-squares fit of some linear transformation of the residues of the data interpolated onto a $0.05\,\text{Å}^{-1}$ spaced grid. Options include fits on three different axes (original or 'R or Q space') with k^2 or k^3 or k^n scaling (suppressing near-edge and magnifying far-edge structure), and with a variable fitting window in k space. These transformations of the residues do not propagate experimental uncertainties, distorting the accuracies and uncertainties of the original data set. Therefore, such options are significantly flawed and were not used in this investigation.

4. Significance

To investigate current XAFS theory, this work used newly available absolute mass attenuation data for molybdenum of extremely high accuracy. This was made possible by the implementation of a systematic propagation of errors through least-squares analysis. The current analysis techniques were improved by the implementation of a χ^2_r fitting technique.

Models using 16 independent path coefficients produce unphysical model parameters with both the current analysis technique and χ^2_r fitting technique, due in particular to the correlations between parameters. The use of k^3 scaling is not recommended from this work because unphysical scaling of error bars is common, distorting the meaning of the fitted parameters.

The simpler model with a single common path amplitude produced parameters in reasonable agreement with literature values when the fit was windowed to 7 peaks. This appears to constitute a more serious constraint upon the range of validity of the model than previously believed, especially since this is the XAFS spectrum of a monoatomic solid.

The χ^2_r for every fit is over 60, clearly indicating a disagreement between theory and experiment. In the abstract, the experimental error bars could simply be too low by a factor of 7. However, the structured pattern of the residuals is inconsistent with a random noise signature, confirming in fact the quality and error bars of the data (to within a factor of two), and highlighting the theoretical issue raised.

The χ^2_r for the unwindowed fit using the current analysis techniques was 3000. Improved theory for the whole range of data should therefore improve agreement with experimental structure by a further factor of $\sqrt{3000} \simeq 55$.

Acknowledgements

The authors acknowledge the experimental team as well as funding from the ASRP and ARC for this work. We acknowledge the assistance of our collaborators at the Advanced Photon Source including David Paterson and the staff of SRI-CAT and BESSRC-CAT.

References

Bashir, J., Butt, N., Khan, M., Khan, Q., Zhang, B., Yang, N., Ding, Y., Ye, C., 1992. Determination of the Debye–Waller factor of molybdenum by powder neutron diffraction. J. Appl. Crystallogr. 25 (6), 797–799.

Chantler, C., 1995. Theoretical form-factor, attenuation and scattering tabulation for $z = 1-92$ from $e = 1-10$ ev to $e = 0.4-1.0$ MeV. J. Phys. Chem. Ref. Data 24 (1), 71–591.

Chantler, C., 2000. Detailed tabulation of atomic form factors, photoelectric absorption and scattering cross section, and mass attenuation coefficients in the vicinity of absorption edges in the soft X-ray ($Z = 30-36$, $Z = 60-89$, $E = 0.1-10$ keV), addressing convergence issues of earlier work. J. Phys. Chem. Ref. Data 29 (4), 597–1048 ⟨http://physics.nist.gov/PhysRefData/FFast/Text/cover.html⟩.

Chantler, C., Tran, C., Barnea, Z., Paterson, D., Cookson, D., Balaic, D., 2001. Measurement of the X-ray mass attenuation coefficient of copper using 8.85–20 keV synchrotron radiation. Phys. Rev. A 64, 062506.

de Jonge, M., Tran, C., Chantler, C., Barnea, Z., Dhal, B., Cookson, D., Lee, W., Mashayekhi, A., 2005. Measurement of the X-ray mass attenuation coefficient and determination of the imaginary component of the atomic form-factor of molybdenum over the energy range of 13.5–41.5 keV. Phys. Rev. A 71, 032702.

Edwards, J., Speiser, R., Johnston, H., 1951. High temperature structure and thermal expansion of some metals as determined by X-ray diffraction data. 1. platinum, tantalum, niobium, and molybdenum. J. Appl. Phys. 22 (4), 424–428.

Hubbell, J., 1994. Bibliography of photon total cross section (attenuation coefficient) measurements 10 eV to 13.5 GeV, 1907–1993. NISTIR 5437.

Mihelic, A., Kodre, A., Arcon, I., Gomilsek, J., 2004. High-resolution X-ray absorption spectrometry of atomic vapors. Acta Chimica Slovenca 51 (1), 22–28.

Newville, M., 2001. Ifeffit: interactive exafs analysis and feff fitting. J. Synchrotron Radiat. 8, 322–324.

Taylor, A., et al., 1961. The constitution diagram of the molybdenum–hafnium binary system. J. Less Common Metals 3, 265–280.

Tran, C., Chantler, C., Barnea, Z., 2003. X-ray mass attenuation coefficient of silicon: theory versus experiment. Phys. Rev. Lett. 90 (25), 257401.

Wyckoff, R., 1963. Crystal Structures. vol. 3. Wiley, New York, p. 16.

Zabinski, S., Rehr, J., Ankudinov, A., Albers, R., Eller, M., 1995. Multiple-scattering calculations of X-ray-absorption spectra. Phys. Rev. B 52 (4), 2995–3009.